Functionalization of Carbon Surfaces Using the Copper-Catalyzed Diels–Alder Reaction

Denis Ari, Jean-Francois Bergamini, Teresa Rodrigues, Wolfgang Knoll, Charles Cougnon, Essraa Ahmed, Paulius Pobedinskas, Ken Haenen, Nicolas Nuns, Rabah Boukherroub, et al.

Functionalization of carbon surfaces using copper-catalyzed Diels-Alder Reaction

Denis Ari,[1] Jean-Francois Bergamini,[1] Teresa Rodrigues,[2] Wolfgang Knoll, [3,4] Charles Cougnon,[5] Essraa Ahmed,[6,7] Paulius Pobedinskas,[6,7] Ken Haenen,[6,7] Nicolas Nuns,[8] Rabah Boukherroub,[2] Sabine Szunerits,[2,4] Yann R. Leroux[1]**

[1]Univ Rennes, CNRS, ISCR – UMR 6226, F-35000 Rennes, France

[2]Univ. Lille, CNRS, Centrale Lille, Univ. Polytechnique Hauts-de-France, UMR 8520 - IEMN, F-59000 Lille, France

[3]AIT Austrian Institute of Technology GmbH, Biosensor Technologies, 3430 Tulln, Austria

[4]Laboratory for Life Sciences and Technology (LiST), Faculty of Medicine and Dentistry, Danube Private University, 3500 Krems, Austria

[5]Université d'Angers, CNRS UMR 6200, Laboratoire MOLTECH-Anjou, 2 bd Lavoisier, 49045 Angers Cedex, France

[6]Hasselt University, Institute for Materials Research (IMO), Wetenschapspark 1, 3590 Diepenbeek, Belgium

[7]IMEC vzw, Division IMOMEC, Wetenschapspark 1, 3590 Diepenbeek, Belgium

[8]Univ. Lille, CNRS, INRAE, Centrale Lille, Univ. Artois, FR 2638 - IMEC – Institut Michel-Eugène Chevreul, F-59000 Lille, France

ABSTRACT:

We propose here a new method to functionalize carbon materials via a catalyzed Diels-Alder reaction. In a Diels-Alder reaction, carbon materials can be used as a diene or a dienophile. Here, carbon materials are used as dienes and alkyne terminated derivatives as dienophiles. Different carbon materials, i.e. glassy carbon, carbon powder (carbon black), pyrolytic graphite carbon materials and graphene were functionalized by alkyne ferrocene derivatives or perfluoro-tagged alkyne molecules and characterized by electrochemical means, AFM and XPS experiments. This method allows for the rapid functionalization of carbon materials in mild conditions with a high surface coverage.

1. Introduction

Carbon based materials have become widely used in electroanalytical chemistry due to their good electrical conductivity, wide potential range, low background current, low cost and general chemical inertness.[1-4] Surface modification has become essential and a determining factor in the construction of transducers based on carbon materials and more generally in the emerging field of molecular devices.[5-9] Beyond the aim of anchoring specific molecular functionality to carbon surfaces, large efforts have been devoted to the search for robust anchoring groups, which can integrate in a controlled manner onto carbon surfaces and which allow post-grafting approaches, an essential step for selective sensing-based applications.[10-12] A large number of methods to functionalize carbon surfaces have thus been developed over the last 50 years.[13-17] Since its discovery in 1992 by Pinson and coworkers,[18] the (electro) reduction of aryl diazonium salts is among the most popular strategies for adding functionality onto carbon materials via covalent bond formation. Upon reduction of aryl diazonium salts, highly reactive aryl radicals are formed, which interface with the carbon surface. The high reactivity of these intermediates is the driving force for an efficient functionalization of carbon materials, but it is also responsible for its major drawback which is the lack of control of the extent of the reaction, that generally leads to multilayer disordered organic deposits. This is contrary to the well-known self-assembled monolayers (SAMs) on coinage metals for instance,[19] where terminal cysteine and thiol groups form stable and well-ordered SAMs on gold. Alkynes have been shown to be alternative surface ligands not only for the formation of stable Au-C bonds,[20] and formation of Si-C bond on hydrogen-terminated silicon (Si-H),[21] but also for the formation of C-C bonds on carbon materials.[22, 23]

Among the different possibilities that terminal alkynes offer for surface functionalization, copper catalyzed click chemistry,[24] Sonogashira cross-coupling reactions[25, 26] or Glaser reactions,[27] have been largely investigated. More recently Geiger and coworkers proposed a new method that allows the direct use of terminal alkynes to functionalize carbon materials without the need for surface pre-treatment.[22, 23] The approach is based on the activation of terminal alkyne groups by butyllithium (BuLi). The lithium-stabilized carbanion formed can be oxidized in a one electron process to the corresponding ethynyl radical, which then reacts with the surface. The spontaneous interaction of lithium-activated alkynes with the surface,[28] as well as the direct anodic oxidation of terminal alkynes at higher potential are other possibilities offered by this approach.[29-31]

In addition, terminal alkynes are good dienophiles in Diels-Alder reactions. The Diels-Alder reaction is an efficient alternative method to functionalize carbon materials, with several reviews available on the subject.[32-34] Interestingly, work carried out by Haddon *et al.* show that graphite and graphene interfaces can act as a diene or a dienophile in Diels-Alder reaction;[35] similar observations have been made by Abets *et al.* using carbon nanotubes.[36] However, despite its efficiency and versatility, the surface-based Diels-Alder reaction generally requires long reaction times, up to a few days,[37-39] and the use of elevated temperatures to drive the reaction successfully.[40-42] The use of specific solvents, such as deep eutectic solvents,[43] microwaves[44] or ultrasonication[45] have all successfully accelerated the functionalization rate and thus made this surface reaction of higher utility.

In this study, we propose to use a copper-catalyzed Diels-Alder reaction to modify carbon-based materials with terminal alkynes via the dienophile character of the ligand. We show that

the presence of Cu(I) alone, formed *in-situ* by the reduction of Cu(II) using ascorbic acid, increases the reaction rate with the carbon interface, without the requirement of elevated temperatures or long reaction times. Using ferrocene and perfluoro alkyne derivatives as model alkynes leads to self-limited monolayers on carbon surfaces with strong C-C bonds and in mild conditions allowing the functionalization of carbon materials with a wide range of molecules or biomolecules.

2. Material and Methods.

2.1. Chemicals and reagents.

All commercially available reagents were used as received. The glassy carbon electrode (3 mm in diameter), basal and edge pyrolytic graphite electrodes (PGE) were purchased from IJ Cambria. Carbon black, copper(I) trifluoromethanesulfonate toluene complex, ascorbic acid, ethylenediaminetetraacetic acid (EDTA) and copper sulfate pentahydrate were purchased from Alfa Aesar. Ethynylferrocene and copper(II) trifluoromethanesulfonate were purchased from Fluorochem. PTFE membranes (47 mm in diameter and 0.45 μm in pore size) were purchased from Sartorius. Sodium acetylene, dichloromethane, magnesium sulfate, 1H-Perfluorooct-1-yne, THF, tetrabutylammonium hexafluorophosphate ($TBAPF_6$), *n*-BuLi, Ethyl chloroformate, Et_2O, EDTA) were purchased from Sigma-Aldrich.

Highly conductive B-doped Si(100) substrates were exposed to a reactive oxygen gas plasma in order to remove hydrocarbon contamination and achieve high nanodiamond (ND) seeding density using the process described elsewhere.[46] The substrates were ND seeded by drop-casting a water-based ND colloid onto the surface and covering it completely, followed by spinning the sample at 4000 rpm and flushing with deionized water for 15 s, and finally spinning for 30 s to dry the surface. The boron-doped nanocrystalline diamond BDD layers were synthetized in an

ASTeX 6500 series microwave plasma-enhanced chemical vapor deposition (MW PE CVD) reactor. The base pressure was ~10^{-6} Torr. During the deposition the substrate temperature was kept at 800°C using 4000 W of MW power and total gas pressure of 40 Torr. The total gas flow rate was 500 sccm, where CH_4 constituted 1% in H_2. The CVD diamond was B-doped by introducing trimethylboron (TMB) into the gas phase with a B/C ratio of 20000 ppm. The diamond growth lasted for 60 min and 150 nm thick BDD thin films were grown.

Graphene electrodes were formed by deposition of in-house made graphene onto thin gold films deposited on glass (5 nm Cr/50 nm Au) as reported previously by our group[47] on interdigitated gold electrodes. In short, the monolayer graphene used in this work is grown by chemical vapor deposition (CVD) on commercial Cu foil followed by wet transfer onto the thin gold film electrode using polymethylmethacrylate (PMMA) as supporting layer.

2.2. Synthesis of different ethynyl-terminated molecules

2.2.1. 11-undecenylferrocene.

In a Schlenk, 510 mg of 11-bromoundecylferrocene[48] was introduced and dissolved in DMF (10 mM). Sodium acetylene (600 µL, 18% in xylene) was added and the solution stirred at room temperature for one hour. After addition of water, the organic phase was extracted with dichloromethane and then dried with magnesium sulfate. The crude product was purified by flash chromatography on silica using petroleum ether as eluent. Yield: 87% (385 mg). RMN ^{1}H (300 MHz, $CDCl_3$): ^{1}H NMR (300 MHz, $CDCl_3$) δ 4.18 (sb, 9H), 2.28 – 2.13 (m, 4H), 1.93 (t, J = 2.7 Hz, 1H), 1.40 (m, J = 73.4 Hz, 16H).

2.2.2. Ethyl 14-ferrocenyltetradec-2-ynoate.

n-BuLi (105 µL, 2.5 M in hexane, 0.26 mM, 1 eq) was added to a THF solution of 11-undecenylferrocene (95 mg, 0.26 mM, 1eq) at -78 °C , and the reaction stirred for 30 minutes at -78 °C. Ethyl chloroformate (25 µL, 0.26 mM, 1 eq) was added dropwise, the reaction warmed to room temperature and stirred for 2 h. The reaction was quenched with deionized water at 0°C and extracted with Et_2O. The combined organic extracts were washed with brine and dried over magnesium sulfate. The crude product was purified by flash chromatography using petroleum ether:dichloromethane (7:3) as eluent. Yield 60% (69 mg). ^{1}H NMR (300 MHz, $CDCl_3$) δ 4.77-4.31 (m, 9H), 4.22 (q, *J* = 7.1 Hz, 2H), 2.32 (t, *J* = 7.0 Hz, 2H), 1.58 (p, *J* = 7.0 Hz, 2H), 1.47-1.19 (m, 20H).

2.3. Catalyzed Diels-Alder protocol

Carbon substrates (BDD, graphene and GCE) were immersed in a 5 mL THF solution containing 5 mg of dienophile. 2.5 mL of 10^{-2} M copper sulfate solution was then added. The solution was stirred and 2.5 mL of 2.10^{-2} M sodium ascorbate solution added dropwise. The solution was stirred for one hour at room temperature after which the carbon substrates were dipped and stirred in a 10 g L^{-1} EDTA solution for 15 min. The substrates were rinsed with water, acetone and dried under a flow of Argon.

For carbon powder modification, 100 mg of carbon black were dispersed in 75 mL of THF containing 17.5 mg (0.01 eq) of ethynylferrocene. Copper sulfate (37.5 mL of 10^{-2} M solution in water) was added followed by addition of sodium ascorbate (37.5 mL of 2.10^{-2} M solution in water). The solution was stirred for one hour at room temperature and then filtered onto a PTFE membrane and washed with acetone (3 × 150 ml). The modified carbon powder was re-dispersed into 150 mL of 10 g L^{-1} EDTA solution and stirred for 30 min before being filtered again onto a

new PTFE membrane. The modified carbon powder was finally washed with water (3 × 150 mL) and acetone (3 × 150 mL) and dried overnight under vacuum.

A carbon ink was made using 45 mg of (modified) carbon powder and 5 mg of PMMA in 1 mL of chloroform. After stirring for two hours, 75 µL of the carbon ink was deposited onto Pt collectors and dried overnight at 70°C before it was used in a home-made 2-electrode cell Swagelok type for electrochemical analysis.

All experiments were repeated on three different electrodes each time and an average surface coverage was determined. Each linear fitting presented in this study has $r^2 > 0.997$, except for carbon black deposits, for which $r^2 = 0.987$.

2.4. Electrochemical experiments.

Electrochemical measurements were performed using a conventional three-electrode system comprising carbon materials as working electrodes, a platinum wire or mesh (IJ Cambria) as an auxiliary electrode, and a saturated calomel electrode (SCE) (Metrohm) as a reference. The potentiostat was an Autolab PGSTAT 302N (Metrohm). Electrochemical analyses of the carbon powder were performed in a home-made 2-electrode cell Swagelok type using Origaflex OGF500 (Origalys) potentiostat. Glassy carbon electrodes were polished on 5 µm SiC abrasive paper and thoroughly rinsed before use.

2.5. X-ray Photoelectron spectroscopy (XPS).

X-ray photoelectron spectroscopy (XPS) characterizations were recorded with an SPECSLAB II (Phoibos-Hsa 3500 150, 9 channels) spectrometer using an Al Kα source (E = 1486.6 eV) operating at 12 kV, pass energy of 40 eV, 0.1 eV energy step and acquisition time of 1 s per

point. The residual pressure inside the analysis chamber was ~1 × 10^{-8} Torr. All XPS peaks were referenced according to the adventitious C1s peak at 284.5 eV.

2.6. Raman spectroscopy.

Raman spectroscopy measurements on graphene were performed on a LabRam HR Micro-Raman system (Horiba Jobin Yvon, France) combined with a 473 nm laser diode as excitation source. Visible light was focused by a 100x objective. The scattered light was collected by the same objective in backscattering configuration, dispersed by an 1800 mm focal length monochromator and detected by a CCD. Raman spectra of nanocrystalline diamond were measured using Reinshaw inVia Raman Microscope with a laser of 532 nm.

2.7. Atomic Force Microscopy (AFM) Experiments.

All atomic force microscopy (AFM) experiments have been performed on an NT-MDT Ntegra microscope. Scratching experiments were performed in order to estimate the thickness of the organic layers.[49] The term "AFM scratching" is used here to describe intentional damage to a modification layer on a relatively hard substrate. Scratches were realized in contact mode applying a sufficient force to sweep organic material. After the scratching step, the scratched square zones were imaged in semi-contact mode and analyzed by Gwyddion open-source software.[50] The heights of organic layers were extracted from the depths of the scratched zones averaged on different profiles. The scratching experiments were also run on bare surfaces with the same tip and same force applied to determine if the tip was scratching the substrate. The eventual scratch depth was then subtracted from the depth measured for the functionalized surfaces.

2.8. Time-of-Flight Secondary Ion Mass Spectrometry (ToF-SIMS) Experiments.

ToF-SIMS experiments were performed using a TOF.SIMS 5 spectrometer (ION-TOF GmbH Germany) equipped with a bismuth liquid metal ion gun (LMIG) for primary ions. Bi^{3+} primary ion beam was used (25 keV, 0.25 pA) for data acquisition. An area of 500 x 500 mm² was analyzed (128 x 128 pixels and 100 scans). The total fluence did not amount up to 10^{12} ions/cm² ensuring static conditions. Charge effects were compensated by means of a 20 eV pulsed electron flood gun. With a cycle time of 100 μs, data were collected over a mass range m/z = 0-800 for both positive and negative secondary ions.

3. Results and Discussion.

3.1. Catalyzed Diels-Alder reaction as surface reaction.

Scheme 1 shows a schematic representation of the catalyzed Diels-Alder reaction on carbon materials with the different ligands employed. These different alkyne derivatives were selected in order to understand in detail the surface reaction taking place in this study. Diels-Alder reactions are well-known to be catalyzed by copper ions[51] and this approach was followed here using copper sulfate ($CuSO_4$) as a source of copper(II) that is *in-situ* reduced by sodium ascorbate to copper(I). First, glassy carbon electrodes (GCE) were functionalized using ethynylferrocene as dienophile in a catalyzed Diels-Alder reaction for one hour.

Scheme 1. Schematic representation of the catalyzed-Diels-Alder reaction on carbon surfaces.

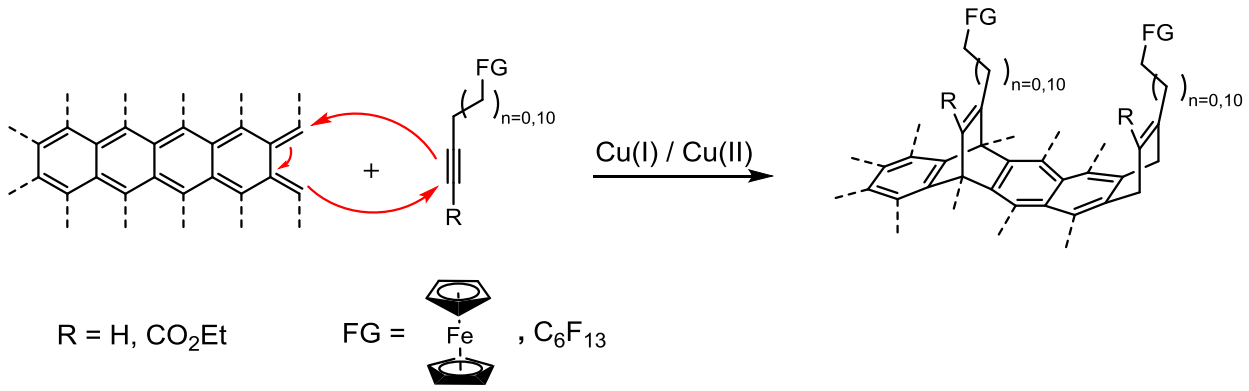

Figure 1a shows the cyclic voltammogram responses of a functionalized GCE in an electrolytic dichloromethane solution containing 0.1 M of tetrabutylammonium hexafluorophosphate ($TBAPF_6$) at different scan rates, from 0.1 $V.s^{-1}$ to 1 $V.s^{-1}$. The presence of the ferrocene redox couple is clearly observed at 0.53 V vs SCE. The peak-to-peak separation (ΔE) at 0.1 $V.s^{-1}$ is ΔE = 46 mV, below the theoretical ΔE = 59 mV for a freely diffusive electroactive species, indicating immobilization of ferrocenyl moieties onto the GCE. The variations of the anodic and cathodic peak current density scale linearly with the scan rate (**Figure 1b**), underlining the surface confined character of ferrocene. The electrochemical signal is quite broad in these experiments but this can easily be explained by the roughness of the carbon electrode, leading to ferrocenyl moieties being located at various distances, which results in a range of formal electrode potentials.[52, 53] The surface coverage, Γ, of ferrocenyl moieties immobilized onto the carbon surface has been estimated using the following equation:

$$\Gamma = 4aRT/F^2 \qquad (1)$$

with a the slope of the linear variation of the peak current density versus the scan rate (**Figure 1b**), R the universal gas constant, T the temperature, and F the Faraday constant. Considering a temperature of 298 K, a ferrocene surface coverage of $\Gamma = (4.79 \pm 0.17) \times 10^{-11}$ $mol.cm^{-2}$ is

estimated. Considering the theoretical maximum surface coverage of ferrocenyl moieties of $\Gamma = 4.5 \times 10^{-10}$ mol.cm^{-2}, [31] a ten times lower surface coverage is achieved under these conditions.

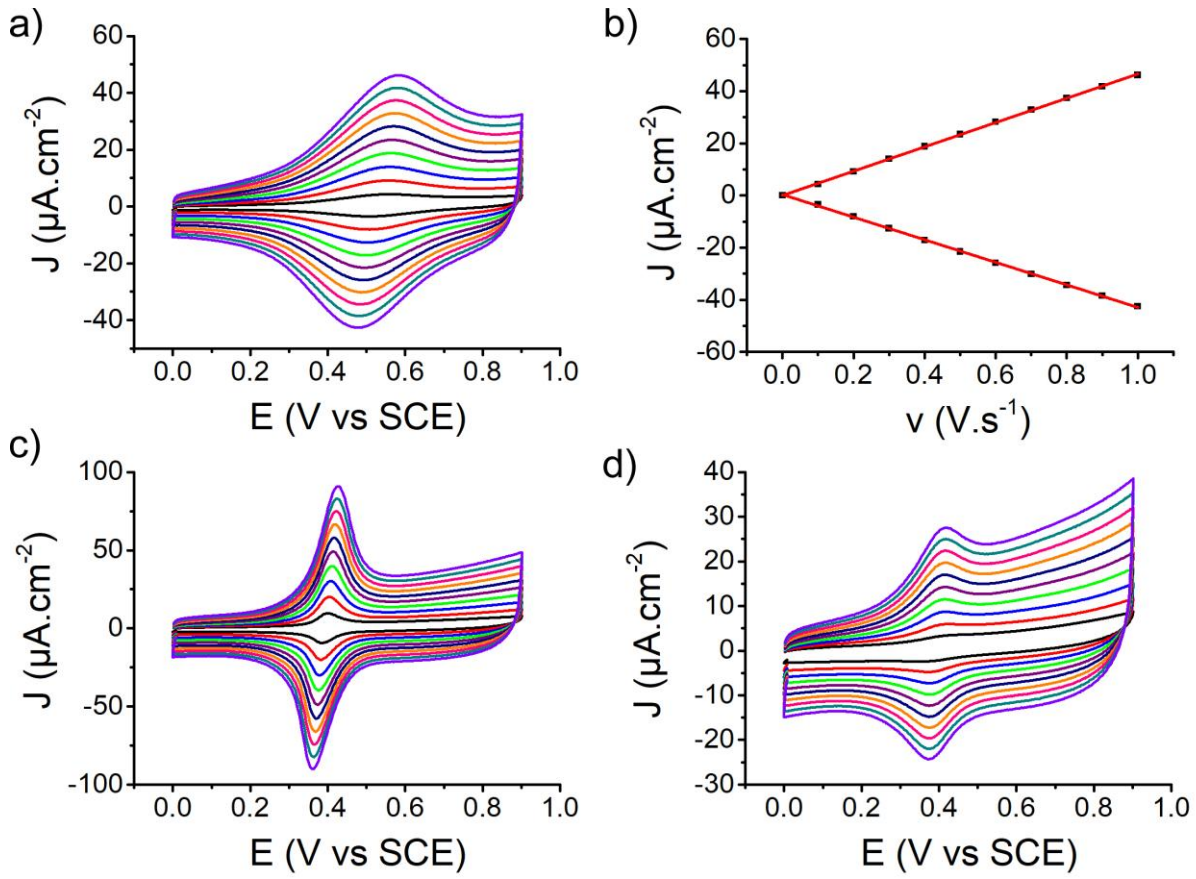

Figure 1. Cu(I) catalyzed Diels-Alder reaction on glassy carbon electrodes using different ferrocenyl dienophiles. Cyclic voltammograms of GCE functionalized with (a) ethynylferrocene, (c) **Fc-(CH$_2$)$_{11}$-Eth-CO$_2$Et**, (d) **Fc-(CH$_2$)$_{11}$-Eth** using the catalyzed Diels-Alder method at different scan rates (100 mV.s^{-1} to 1000 mV.s^{-1}) in a dichloromethane solution containing 0.1 M $TBAPF_6$. b) Variation of the anodic and cathodic peak current density of ethynylferrocene modified GCE with scan rate. Red lines are linear fitting curves.

3.2. Effect of activation of the dienophile.

To better understand this catalyzed surface reaction, different alkyne derivatives were used. Indeed, in contrast to retro-Diels-Alder reactions, electron deficient dienophiles are required for a Diels Alder reaction. In our case we assume that the carbon surfaces serve as dienes and ferrocenyl alkyne derivatives as dienophiles. A set of two different dienophiles, 11-undecenylferrocene (**Fc-$(CH_2)_{11}$-Eth,** R = H and FG = ferrocene in **Scheme 1**) and ethyl 14-ferrocenyltetradec-2-ynoate (**Fc-$(CH_2)_{11}$-Eth-CO_2Et,** R = CO_2Et and FG = ferrocene in **Scheme 1**) were investigated in the following studies. The enolate CO_2Et electron withdrawing group renders the alkyne electron deficient, while the long alkane carbon chain between the ethynyl group and the ferrocenyl moiety ensures no electronic communication between them. **Figures 1c and 1d** show the cyclic voltammogram responses of GCE modified with each ligand in the same manners as in **Figure 1a**. It is notable that the carbon electrodes functionalized with **Fc-$(CH_2)_{11}$-Eth** and **Fc-$(CH_2)_{11}$-Eth-CO_2Et** present narrower reversible electrochemical signals than carbon electrodes modified with ethynylferrocene, a result of flexibility and decoupling of the ferrocenyl moieties from the carbon surfaces using the long alkane chain. In both cases, the reversible electrochemical signal is centered at 0.39 V vs SCE, in accordance with the formal potential of an alkane-modified ferrocene derivatives, with a ΔE = 15 mV at 0.1 $V.s^{-1}$ for **Fc-$(CH_2)_{11}$-Eth-CO_2Et** and ΔE = 44 mV at 1 $V.s^{-1}$ for **Fc-$(CH_2)_{11}$-Eth** respectively. The surface coverage of ferrocenyl moieties is increased to $\Gamma = (3.31 \pm 0.22) \times 10^{-10}$ $mol.cm^{-2}$ when using the electron deficient dienophile **Fc-$(CH_2)_{11}$-Eth-CO_2Et**, being close to the theoretical maximum surface coverage. This differs to **Fc-$(CH_2)_{11}$-Eth,** whereas it is only $\Gamma = (2.78 \pm 0.16) \times 10^{-11}$ $mol.cm^{-2}$. The variation of the anodic and cathodic peak current density are linear with the applied scan rate in the 0.1 $V.s^{-1}$ to 1 $V.s^{-1}$ range on both functionalized carbon electrodes (**Figure S2 and S3**), confirming the good immobilization of the ferrocenyl moieties onto the carbon surfaces via this

surface reaction. The difference observed in surface coverages between activated and non-activated alkyne derivatives suggests that the surface reaction study here is a catalyzed Diels-Alder reaction.

3.3. Effect of copper catalysts.

To shed light on the importance of the catalyst and its redox state, we performed the same Diels-Alder surface reaction in the absence of copper ions in the solution. As can be seen on **Figure 2a**, 10 times lower electrochemical response ($\Gamma = (3.26 \pm 0.02) \times 10^{-11}$ mol.cm^{-2}) can be observed in the case of **Fc-(CH$_2$)$_{11}$-Eth-CO$_2$Et** modified GCE, while almost no electrochemical signal was detectable under these non-catalytic conditions using **Fc-(CH$_2$)$_{11}$-Eth** as dienophile (**Figure 2b**). In the literature, both copper(I) and copper(II) ions have been shown to efficiently catalyze numerous Diels-Alder reactions.[51] Hence, we performed the same reaction with $CuSO_4$ in the absence of ascorbic acid (Cu(II) as catalyst). Similar results are obtained for **Fc-(CH$_2$)$_{11}$-Eth-CO$_2$Et** modified GCE, compared to experiments realized with copper(I) catalyst, while no ferrocene signature is observed using **Fc-(CH$_2$)$_{11}$-Eth** as dienophile. These observations clearly highlight the need of copper catalyst and to activate the dienophile to obtain fast and efficient surface functionalization using the catalyzed Diels-Alder reaction.

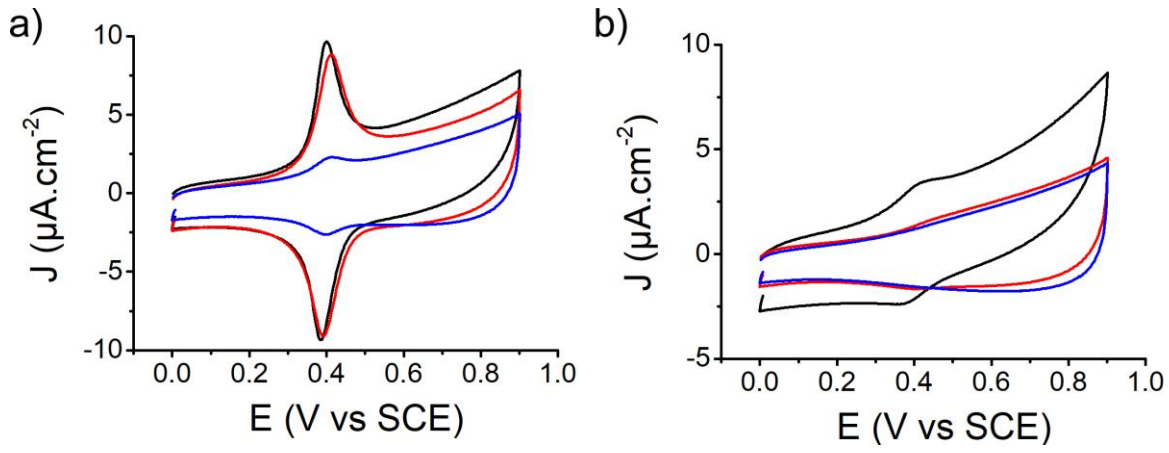

Figure 2. Cyclic voltammograms of glassy carbon electrode functionalized with two different ferrocenyl dienophiles in the absence or presence of copper ions as catalyst. GCE functionalized with (a) **Fc-$(CH_2)_{11}$-Eth-CO_2Et** and (b) **Fc-$(CH_2)_{11}$-Eth** using copper(I) (black curves), copper(II) (red curves) as catalysts in a catalyzed Diels-Alder method and without catalyst (no copper ions, blue curves) in a dichloromethane solution containing 0.1 M $TBAPF_6$.

3.4. Surface characterization.

Atomic force microscopy (AFM) was used to characterize the topography and the thickness of the organic layer grafted on carbon electrodes. For this purpose, as GCEs show high surface roughness (typically around 0.5 µm) we used pyrolyzed photoresist films (PPF) as carbon surfaces for AFM experiments which present similar reactivity than GCE but a lower surface roughness (around 0.5 nm). AFM images of PPF substrates functionalized with **Fc-$(CH_2)_{11}$-Eth-CO_2Et** were recorded. These images were performed in ambient conditions (in air and at room temperature) and present a classic globular structure of the organic deposit at the nanometer scale (**Figure 3a**).[12] To estimate the thickness of the organic deposit, scratching experiments were conducted.[49] Briefly, it consists in the intentional damage of the organic film by the AFM tip to carve out a square trench. For this purpose, 0.5 × 0.5 µm scratches were made by moving the tip

in contact mode with a sufficient force to sweep the organic layer. The same scratching procedures were done on the bare PPF surface with the same tip and same applied force and confirmed that scratching of the PPF substrate did not occur. The images shown in **Figure 3** were acquired in semi-contact mode, and representative line profiles through scratch are also shown in inset. Note that loose debris from the scratch often create AFM tip-surface tracking problems resulting in lower image quality. From the line profile, such as the one shown in **Figure 3b**, we can estimate an average thickness of the organic deposit close to 1.0 ± 0.1 nm. This value has to be compared to the 2.0 nm theoretical length of **Fc-$(CH_2)_{11}$-Eth-CO_2Et** which is estimated using Chem 3D software.[54] Whereas this low thickness value of the organic deposit may be surprising, it should be considered that the long alkane chain of this molecule in air should collapse onto the carbon surface. Hence, this result is coherent with the deposition of a monolayer organic film, as expected for a Diels-Alder reaction. Furthermore, a slight increase in surface roughness from 0.25 nm to 0.58 nm, for bare surface and functionalized surface respectively, supports a monolayer deposit.

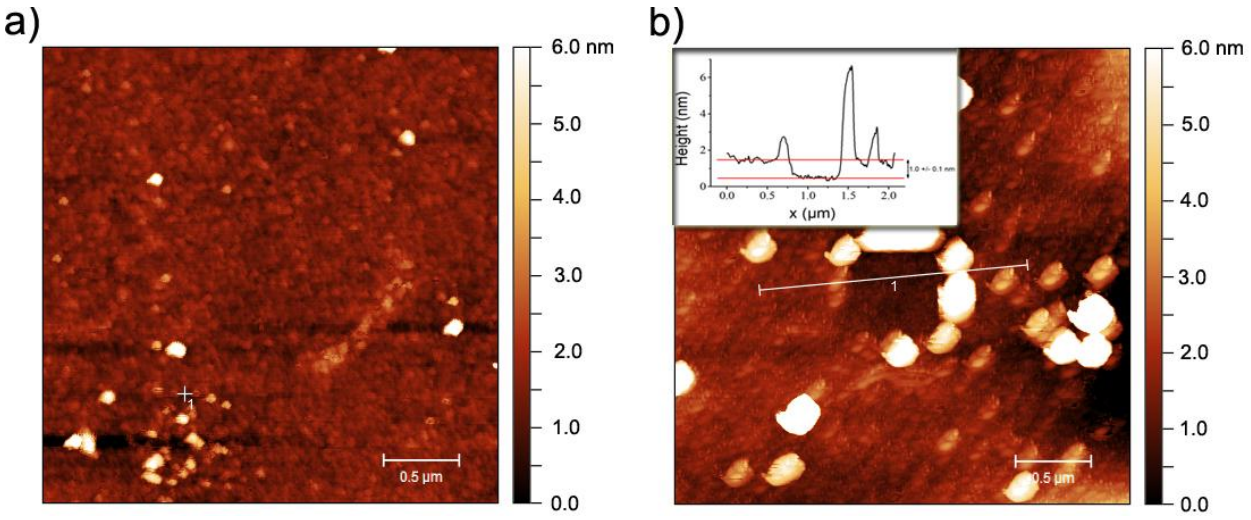

Figure 3. Atomic force microscopy (AFM) imaging. (a) AFM image of pyrolyzed photoresist film (PPF) functionalized with **Fc-$(CH_2)_{11}$-Eth-CO_2Et** using copper(I) as catalysts in a catalyzed Diels-Alder surface reaction. (b) Example of AFM scratching experiment on the same modified PPF sample. Insert: line profile.

To further evidence the monolayer deposition of the organic film by Diels-Alder reaction, the functionalized glassy carbon electrodes were analyzed by time-of-flight secondary ion mass spectrometry (ToF-SIMS).[55] In ToF-SIMS experiments, the samples are bombarded by Bi^{3+} and secondary ions are detected by mass spectroscopy. The detected masses are molecular fragments desorbed from the surface substrate. Figure 4 shows the mass spectrum in positive mode obtained on functionalized glassy carbon using **Fc-$(CH_2)_{11}$-Eth-CO_2Et** as dienophile in catalyzed Diels-Alder reaction. The predominant peak observed at m/z 436.17 corresponds to **Fc-$(CH_2)_{11}$-Eth-CO_2Et**$^+$ fragments. Another predominant peak observed at m/z 473.30 is attributed to $C_{29}H_{37}FeO_2^+$ and highlights the strong interaction between the substrate and the modifier by covalent bonds where fragments of the carbon substrate (carbon atoms) are desorbed with the molecular modifier. No other peaks are detected at higher m/z confirming the monolayer character of the grafted organic film, ruling out any oligomerization or polymerization reactions at the substrate surface.

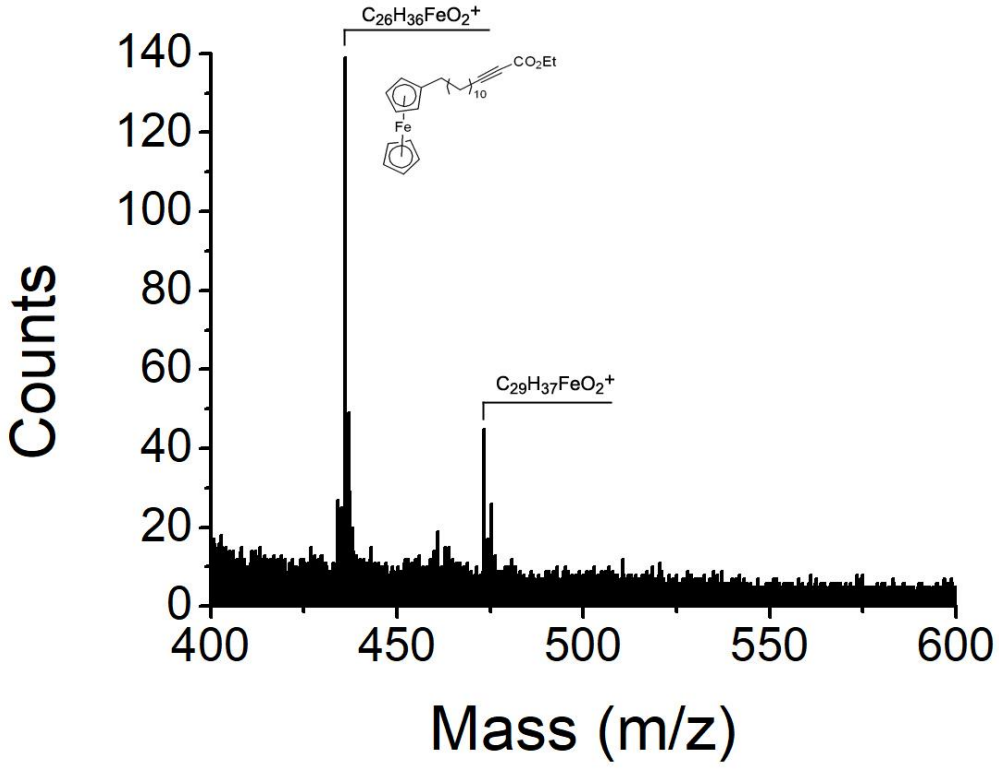

Figure 4. ToF-SIMS spectrum of glassy carbon substrate functionalized with Fc-$(CH_2)_{11}$-Eth-CO_2Et using copper(I) as catalysts in a catalyzed Diels-Alder in positive mode.

3.5. Functionalization of other carbon surfaces.

3.5.1. Pyrolytic graphite electrodes.

Encouraged by the possibility of modifying GCEs by a catalyzed Diels-Alder reaction, we wanted to see if this reaction could be generally applied to other carbon materials. **Figure 5a** and **5b** show the cyclic voltammogram responses of functionalized basal and edge pyrolytic graphite electrodes (PGE) which is similar to highly oriented pyrolytic graphite (HOPG). While reversible electrochemical signals corresponding to grafted ferrocene units are observed at 0.57 ± 0.01 V vs SCE with a ΔE = 28 ± 1 mV at 0.1 $V.s^{-1}$, and a linear correlation between current density and scan rate (**Figure S4 and S5**), the surface coverage of ferrocene on basal PGE is Γ =

(3.94) ± 0.08 × 10^{-11} mol.cm^{-2} while on edge PGE it equals to Γ = (1.20 ± 0.02) × 10^{-10} mol.cm^{-2}. There is a long debate about the difference of reactivity of basal plan and edges when considering HOPG materials. Without suggesting any differences about the intrinsic electron transfer kinetic of basal and edge PGEs, it is clear in our experiments that the catalyzed Diels-Alder reaction is more efficient onto edge PGE. This can be due to the configuration of the electrode surface where in the case of the edge PGE, expansion of the graphitic material can occur easily upon functionalization,[56] which is not the case when considering the basal plane.

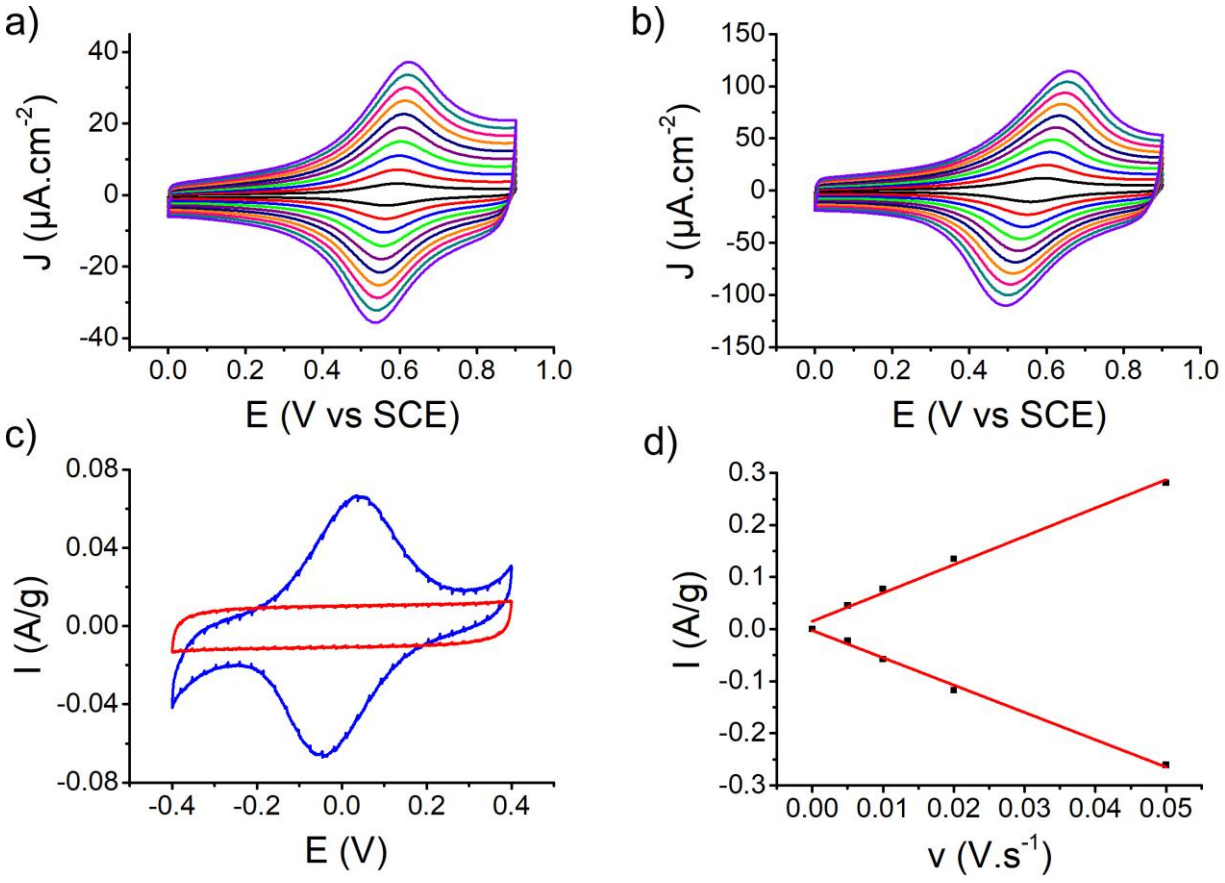

Figure 5. Cyclic voltammograms of ethynylferrocene modified pyrolytic graphite electrodes and carbon powder using the Cu(I) catalyzed Diels-Alder reaction: (a) basal pyrolytic

graphite electrode and (b) edge pyrolytic at different scan rates (100 $mV.s^{-1}$ to 1000 $mV.s^{-1}$). (c) Unmodified (red curve) and functionalized (blue curve) carbon powder (carbon black acetylene) at 10 $mV.s^{-1}$ in a two-electrode configuration. (d) Variation of the anodic and cathodic peak current density of ethynylferrocene modified carbon powder with scan rate. Red lines are linear fitting curves.

3.5.2. Carbon powder electrode.

Carbon powders were also considered as another carbon material to modify via the catalyzed Diels-Alder reaction. To assess the electrochemical response of ferrocene-functionalized carbon powder, it was deposited onto platinum (Pt) collectors via a carbon ink using poly(methyl methacrylate) (PMMA) as binder, and tested in a two-electrode configuration. Whereas unmodified carbon powder only shows capacitive current (**Figure 5c**, red curve), a reversible electrochemical signal is recorded onto functionalized carbon powder (**Figure 5c**, blue curve), centered at 0 V due to the two-electrode configuration, with current density as high as 0.065 A/g at 10 $mV.s^{-1}$. The variation of the anodic and cathodic peak current densities are linear with the applied scan rate in the 0.01 $V.s^{-1}$ to 0.05 $V.s^{-1}$ range (**Figure 5d**). The scan rate range where linearity is observed is shorter than for planar electrodes due to counter-ion mobility in the carbon deposit, as is observed in carbon supercapacitors for instance.

3.5.3. Graphene based electrodes.

The last sp^2 hybridized carbon material investigated was graphene. As graphene is known to be less reactive than other carbon materials, we first increased the reaction time to 24 h. **Figure 6a** shows the CV responses of ethynylferrocene modified graphene in an electrolytic ethanoic

solution containing 0.1 M of lithium perchlorate ($LiClO_4$) at different scan rates, from 0.1 $V.s^{-1}$ to 0.5 $V.s^{-1}$. The ferrocene unit is clearly observed, with a peak-to-peak separation ΔE = 65 mV. The anodic and cathodic peak current density scale linearly with the scan rate (**Figure 6b**) underlining the surface confined character of the ferrocene moieties. The surface coverage, Γ, of ferrocenyl moieties immobilized onto the graphene surface was estimated using equation (1) and equal to $\Gamma = (1.12 \pm 0.45) \times 10^{-11}$ $mol.cm^{-2}$, in the order of the surface coverage obtained on GCE. We further opted to investigate the Diels-Alder reaction using 1H-perfluorooct-1-yne as dienophile as it is well adapted for X-ray photoelectron (XPS) surface analysis. As 1H-perfluorooct-1-yne is an inactivated dienophile, we notice that its immobilization onto carbon materials is achieved in a time dependent manner (See supporting information). Hence, we performed the functionalization of graphene samples over different durations of 2 h and 24 h total reaction time.

Table 1. XPS analysis of graphene interfaces modified with 1H-perfluorooct-1-yne (5 mM) in THF for 2 or 24h in the absence or presence of $CuSO_4$ (10 mM) and sodium ascorbate (20 mM).

Sample	C1s (%)	O1s (%)	F1s (%)
Bare graphene	95.50	4.50	0.00
Graphene – 2 h	73.20	19.40	7.40
Graphene – 24 h	68.13	21.62	10.25
Graphene – 24 h without copper	79.97	20.03	0.00

XPS analyses were performed before and after functionalization of graphene materials by the catalyzed Diels-Alder reaction using 1H-perfluorooct-1-yne. Compared to bare graphene

samples, a new peak at 689.5 eV is observed in the XPS survey spectrum (**Figure S7**) and is attributed to the F1s core level, corresponding to CF_2-CF_2 and the CF_3 chain end group (**Figure 6c**). High resolution C1s spectra were peak-fitted in several components. After functionalization, bands at 294.1 eV and 291.5 eV (**Figure 6d)** appear and are attributed to the CF_3 chain terminations and CF_2 units of the attached perfluorinated ligands. The other bands at 284.5 eV, 285.0 eV, 286.5 eV and 288.5 eV are assigned to C-sp² and C-sp^3 components and oxygen functions in the form of C-O and C=O, respectively. As seen in Table 1, the atomic % of F1s is time-dependent and reaches a maximum value of 10.25 % after 24 h. Such atomic % correspond to a surface coverage of $\Gamma \sim 8 \times 10^{-11}$ mol.cm^{-2} of 1H-perfluorooct-1-yne immobilized onto monolayer graphene which is in the order of the surface coverages obtained on previous other carbon materials. Concomitantly, oxygen atomic % also increases, but this seems to be due to solvent exposure rather than the functionalization process as such an increase is also observed in control experiments where no copper catalyst is added in the medium. Also, during such control experiment, no peak corresponding to F1s core level can be observed. Finally, the Raman spectrum of functionalized graphene (**Figure S8**) is comparable to that of unmodified graphene (**Figure S6**) with an increase of the I_D/I_G ratio to 0.18 ± 0.02, in accordance with covalent functionalization of graphene materials.[57]

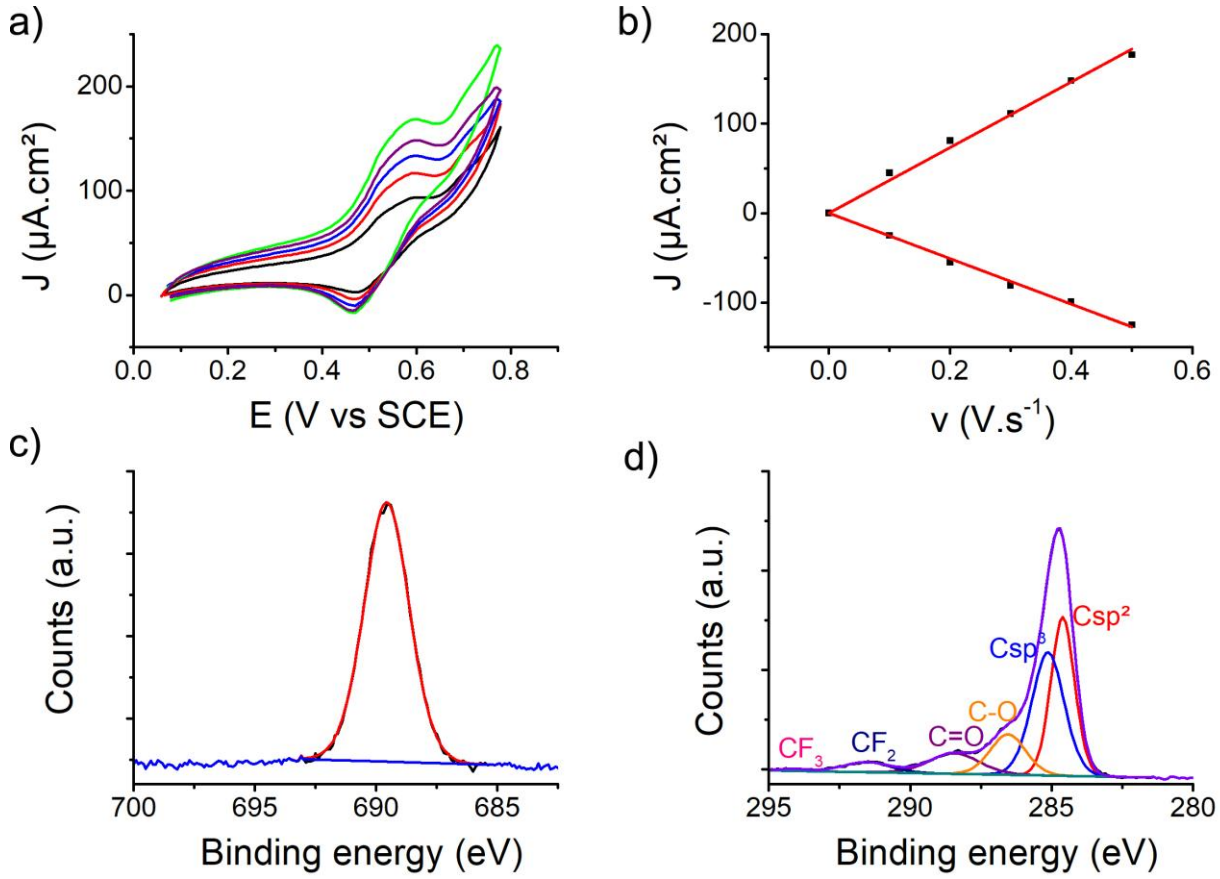

Figure 6. Diels-Alder reaction on graphene: (a) Cyclic voltammograms of ethnylferrocene modified graphene interface for 24 h under catalyzed Diels-Alder conditions in $LiClO_4$ (0.1M)/EtOH at different scan rates (100 mV s^{-1} to 500 mV s^{-1}) . (b) Change of peak current density as a function of scan rate. Red lines are linear fitting curves. (c) High resolution XPS F1s and (d) high resolution XPS C1s spectra of 1H-perfluorooct-1-yne modified graphene samples.

3.6. Effect of the hybridization state of the carbon substrate.

Finally, boron doped diamond (BDD) electrodes (**Figure 7**) were subjected to similar treatment as graphene and the other carbon materials by immersing the interface for 24 h into ethynylferrocene (5 mM) in the presence of $CuSO_4$ (10 mM) and sodium ascorbate (20 mM). While the interface shows diffusion-controlled charge transfer with comparable electrochemical

features as for GCE (**Figure 7,** black curve**)**, no signal due to the presence of linked ferrocene was detected in electrochemical studies (**Figure 7,** red curve). These results were confirmed by XPS analysis of the diamond thin film electrode exposed to ethynylferrocene, where additionally no Fe 2P signature was observed. Diamond is the sole carbon material that possesses only sp^3 carbon atoms. Here, as our BDD films are nanocrystalline, they also contain sp^2 carbon atoms at grain-boundaries (this can be evaluated from Raman spectra, **Figure S9**). Looking from the surface perspective, the amount of Csp^2 *vs* Csp^3 is negligible. Hence, this type of carbon material cannot serve as diene in a Diels-Alder reaction, confirming the nature of the reaction observed in this study.

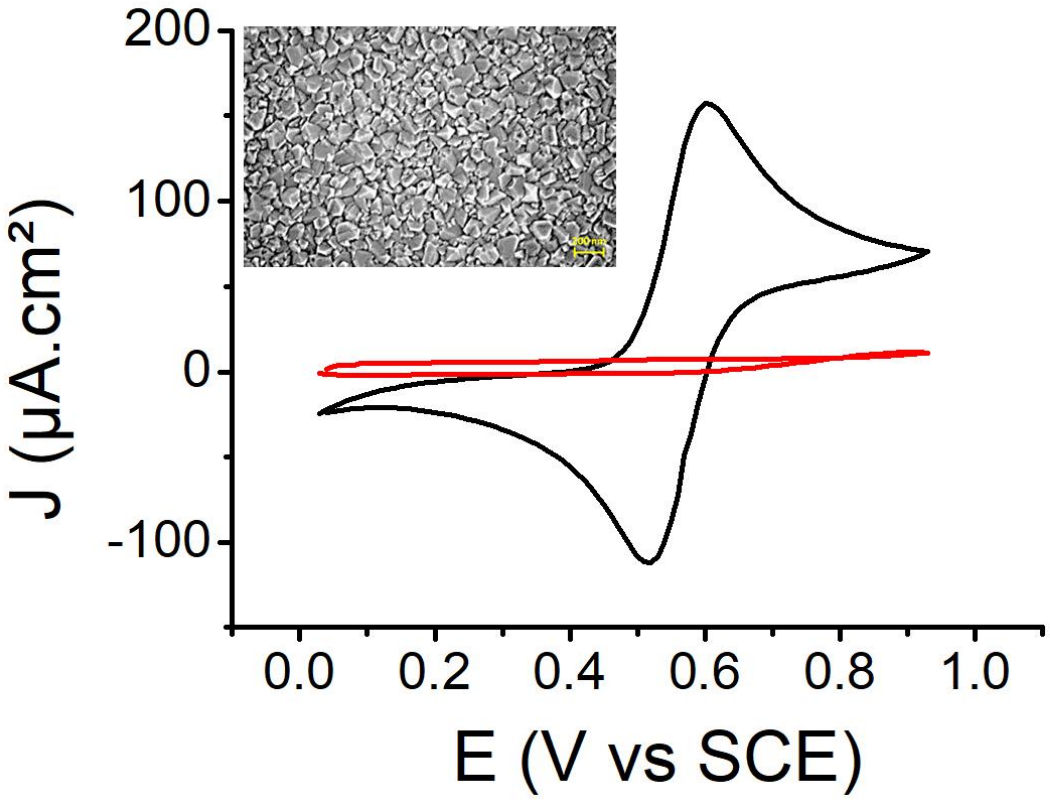

Figure 7. Cu catalyzed Diels-Alder reaction on boron doped diamond electrodes: cyclic voltammograms of ethnylferrocene (5 mM) on a bare BDD electrode in an electrolyte ethanoic

solution containing 0.1 M $LiClO_4$ (black curve) at 0.1 V s^{-1} and after immersion for 24 h into ethynylferrocene (5 mM) in the presence of $CuSO_4$ (10 mM) and sodium ascorbate (20 mM) (red curve). Insert: image of BDD electrode.

3.7. Thermal and electrochemical stability of the functionalized carbon materials.

As fluorine atoms serve as a good XPS tag, the stability of the functionalized substrates were tested using 1H-perfluorooct-1-yne as modifier and PPF as carbon substrates. XPS experiments are presented in supplementary information and their analyzes in Table 2. First, functionalized carbon substrates were heated at 100°C in a toluene solution for one hour. XPS experiments were performed before and after thermal stability tests. From the survey spectrum of the functionalized carbon materials before thermal treatment, we can extract the atomic % of F1s which is equal to 4.1 %. After thermal treatment, this atomic % decreases to 1.8 %, corresponding to a 2.3 fold decrease of surface coverage of the modifier onto the carbon substrate. Such a decrease in surface coverage during thermal treatments is not surprising and corresponds to a retro Diels-Alder reaction. Furthermore, electrochemical stability of the grafted layer was tested on the same sample. In a typical cyclic voltammetry experiment, the functionalized substrate was used as working electrode (with platinum mesh as counter electrode) and its potential was switched between -2.0 V and +1.7 V vs SCE in a 0.1 M tetrabutylammonium hexafluorophosphate dichloromethane solution. XPS measurements performed after this electrochemical stability test show again a 2.8 fold decrease of the surface coverage of the modifier from the survey spectra. As before, the C1s region could be decomposed onto various components of which bands at 292.3 eV and 293.3 eV corresponding to CF2 and CF3 units of the modifier. Theoretically, the atomic ratio between CF2 and CF3 is expected to be 5 and is close to the experimental values obtained on initial (5.4) and thermally

treated (4.8) functionalized carbon substrates. This atomic ratio decreases to 4 when considering electrochemically treated functionalized carbon substrates, highlighting a degradation of the molecular structure of the grafted modifiers. Hence, whereas the decrease in surface coverage of the modifier by thermal treatment is due to chemical desorption via retro Diels-Alder reaction, the decrease in surface coverage of the modifier by electrochemical treatment is due to molecular degradation rather than chemical desorption.

Table 2. XPS analysis of PPF substrates modified with 1H-perfluorooct-1-yne for 24h before and after thermal and electrochemical treatments.

	F1s atomic %	CF2/CF3 ratio
Initial functionalized PPF substrate	4.1 %	5.4
After thermal treatment	1.8 %	4.8
After electrochemical treatment	0.6 %	4

4. Conclusions.

We propose in this study to use a copper-catalyzed Diels-Alder reaction as a surface reaction to functionalize carbon materials. This surface functionalization method is short (one hour), utilizes mild conditions, allowing the use of fragile supporting substrates or immobilization of biomolecules and presents high surface coverage. The functionalized carbon surfaces have been characterized by electrochemical means, Raman and X-ray photoelectron spectroscopy (XPS). We demonstrated that numerous carbon materials (glassy carbon, carbon powder, pyrolytic

graphite and graphene) can be functionalized by this method, except nanocrystalline diamond, which presents mostly sp^3 carbon atoms, hence supporting the proposed mechanism for this surface reaction (Diels-Alder reaction). The immobilized molecules are strongly chemisorbed on carbon surfaces as it involves C-C bonds and inherently leads to only monolayer deposits. Other sources of copper(I) and copper(II) have been tested as catalysts for the catalyzed Diels-Alder surface reaction unsuccessfully (copper(II) trifluoromethanesulfonate and copper(I) trifluoromethanesulfonate toluene complex). This is probably due to the steric constraints imposed by the carbon surfaces when compared to catalyzed Diels-Alder reactions in solution.

Declaration of competing interest

The authors declare that they have no known competing financial interests or personal relationships that could have appeared to influence the work reported in this paper.

Acknowledgements

This work was supported by the ANR-22-CE05-0011-03 (HOMERE). Financial support from the Centre National de la Recherche Scientifique (CNRS) is acknowledged. D.A. thanks Ouest Valorisation for financial support. K.H. acknowledges the financially support of the Methusalem NANO network. E.A. is supported by the Research Foundation Flanders (FWO) grant no. G0D4920N. We would like to warmly thank Dr. James Behan for the careful proof-reading of the manuscript for English grammar and spelling.

Appendix A. Supplementary data

Additional experiments including scanning electron microscopy (SEM) images, X-ray photoelectron spectra (XPS), Raman spectra, AFM images and line profiles and electrochemical experiments, plots and simulated curves.

AUTHOR INFORMATION

Corresponding Author

* sabine.szunerits@univ-lille.fr, yann.leroux@univ-rennes1.fr

REFERENCES

(1) Łukaszewicz, J. P. Carbon Materials for Chemical Sensors: A Review. *Sensor Letters* **2006**, *4* (2), 53-98. DOI: 10.1166/sl.2006.020.
(2) Zhao, Q.; Gan, Z.; Zhuang, Q. Electrochemical Sensors Based on Carbon Nanotubes. *Electroanalysis* **2002**, *14* (23), 1609-1613, https://doi.org/10.1002/elan.200290000. DOI: https://doi.org/10.1002/elan.200290000 (acccessed 2022/10/24).
(3) Qureshi, A.; Kang, W. P.; Davidson, J. L.; Gurbuz, Y. Review on carbon-derived, solid-state, micro and nano sensors for electrochemical sensing applications. *Diamond and Related Materials* **2009**, *18* (12), 1401-1420. DOI: https://doi.org/10.1016/j.diamond.2009.09.008.
(4) Li, C.; Thostenson, E. T.; Chou, T.-W. Sensors and actuators based on carbon nanotubes and their composites: A review. *Composites Science and Technology* **2008**, *68* (6), 1227-1249. DOI: https://doi.org/10.1016/j.compscitech.2008.01.006.
(5) Hetemi, D.; Noël, V.; Pinson, J. Grafting of Diazonium Salts on Surfaces: Application to Biosensors. *Biosensors* **2020**, *10* (1), 4.
(6) Rabti, A.; Raouafi, N.; Merkoçi, A. Bio(Sensing) devices based on ferrocene–functionalized graphene and carbon nanotubes. *Carbon* **2016**, *108*, 481-514. DOI: https://doi.org/10.1016/j.carbon.2016.07.043.
(7) Nebel, C. E.; Shin, D.; Rezek, B.; Tokuda, N.; Uetsuka, H.; Watanabe, H. Diamond and biology. *Journal of The Royal Society Interface* **2007**, *4* (14), 439-461. DOI: doi:10.1098/rsif.2006.0196.
(8) Nebel, C. E.; Rezek, B.; Shin, D.; Uetsuka, H.; Yang, N. Diamond for bio-sensor applications. *Journal of Physics D: Applied Physics* **2007**, *40* (20), 6443. DOI: 10.1088/0022-3727/40/20/S21.
(9) Tanaka, M.; Niwa, O. Fabrication of Biosensing Interface with Monolayers. *Analytical Sciences* **2021**, *37* (5), 673-682. DOI: 10.2116/analsci.20SCR06.
(10) Troian-Gautier, L.; Mattiuzzi, A.; Reinaud, O.; Lagrost, C.; Jabin, I. Use of calixarenes bearing diazonium groups for the development of robust monolayers with unique tailored

properties. *Organic & Biomolecular Chemistry* **2020**, *18* (19), 3624-3637, 10.1039/D0OB00070A. DOI: 10.1039/D0OB00070A.
(11) Wu, T.; Fitchett, C. M.; Brooksby, P. A.; Downard, A. J. Building Tailored Interfaces through Covalent Coupling Reactions at Layers Grafted from Aryldiazonium Salts. *ACS Applied Materials & Interfaces* **2021**, *13* (10), 11545-11570. DOI: 10.1021/acsami.0c22387.
(12) Leroux, Y. R.; Fei, H.; Noël, J.-M.; Roux, C.; Hapiot, P. Efficient Covalent Modification of a Carbon Surface: Use of a Silyl Protecting Group To Form an Active Monolayer. *Journal of the American Chemical Society* **2010**, *132* (40), 14039-14041. DOI: 10.1021/ja106971x.
(13) Bélanger, D.; Pinson, J. Electrografting: a powerful method for surface modification. *Chemical Society Reviews* **2011**, *40* (7), 3995-4048, 10.1039/C0CS00149J. DOI: 10.1039/C0CS00149J.
(14) Barrière, F.; Downard, A. J. Covalent modification of graphitic carbon substrates by non-electrochemical methods. *Journal of Solid State Electrochemistry* **2008**, *12* (10), 1231-1244. DOI: 10.1007/s10008-008-0526-2.
(15) Downard, A. J. Electrochemically Assisted Covalent Modification of Carbon Electrodes. *Electroanalysis* **2000**, *12* (14), 1085-1096, https://doi.org/10.1002/1521-4109(200010)12:14<1085::AID-ELAN1085>3.0.CO;2-A. DOI: https://doi.org/10.1002/1521-4109(200010)12:14<1085::AID-ELAN1085>3.0.CO;2-A (acccessed 2022/10/21).
(16) Mallakpour, S.; Soltanian, S. Surface functionalization of carbon nanotubes: fabrication and applications. *RSC Advances* **2016**, *6* (111), 109916-109935, 10.1039/C6RA24522F. DOI: 10.1039/C6RA24522F.
(17) Atif, M.; Haider, H. Z.; Bongiovanni, R.; Fayyaz, M.; Razzaq, T.; Gul, S. Physisorption and chemisorption trends in surface modification of carbon black. *Surfaces and Interfaces* **2022**, *31*, 102080. DOI: https://doi.org/10.1016/j.surfin.2022.102080.
(18) Delamar, M.; Hitmi, R.; Pinson, J.; Saveant, J. M. Covalent modification of carbon surfaces by grafting of functionalized aryl radicals produced from electrochemical reduction of diazonium salts. *Journal of the American Chemical Society* **1992**, *114* (14), 5883-5884. DOI: 10.1021/ja00040a074.
(19) Bain, C. D.; Evall, J.; Whitesides, G. M. Formation of monolayers by the coadsorption of thiols on gold: variation in the head group, tail group, and solvent. *Journal of the American Chemical Society* **1989**, *111* (18), 7155-7164. DOI: 10.1021/ja00200a039.
(20) Kobayashi, N.; Kamei, Y.; Shichibu, Y.; Konishi, K. Protonation-Induced Chromism of Pyridylethynyl-Appended [core+exo]-Type Au8 Clusters. Resonance-Coupled Electronic Perturbation through π-Conjugated Group. *Journal of the American Chemical Society* **2013**, *135* (43), 16078-16081. DOI: 10.1021/ja4099092.
(21) Fabre, B. Functionalization of Oxide-Free Silicon Surfaces with Redox-Active Assemblies. *Chemical Reviews* **2016**, *116* (8), 4808-4849. DOI: 10.1021/acs.chemrev.5b00595.
(22) Sheridan, M. V.; Lam, K.; Geiger, W. E. An Anodic Method for Covalent Attachment of Molecules to Electrodes through an Ethynyl Linkage. *Journal of the American Chemical Society* **2013**, *135* (8), 2939-2942. DOI: 10.1021/ja312405h.
(23) Sheridan, M. V.; Lam, K.; Geiger, W. E. Covalent Attachment of Porphyrins and Ferrocenes to Electrode Surfaces through Direct Anodic Oxidation of Terminal Ethynyl Groups. *Angewandte Chemie International Edition* **2013**, *52* (49), 12897-12900, https://doi.org/10.1002/anie.201307453. DOI: https://doi.org/10.1002/anie.201307453 (acccessed 2022/10/21).

(24) Collman, J. P.; Devaraj, N. K.; Eberspacher, T. P. A.; Chidsey, C. E. D. Mixed Azide-Terminated Monolayers: A Platform for Modifying Electrode Surfaces. *Langmuir* **2006**, *22* (6), 2457-2464. DOI: 10.1021/la052947q.
(25) Müri, M.; Gotsmann, B.; Leroux, Y.; Trouwborst, M.; Lörtscher, E.; Riel, H.; Mayor, M. Modular Functionalization of Electrodes by Cross-Coupling Reactions at Their Surfaces. *Advanced Functional Materials* **2011**, *21* (19), 3706-3714, https://doi.org/10.1002/adfm.201100642. DOI: https://doi.org/10.1002/adfm.201100642 (acccessed 2022/08/30).
(26) Touzé, E.; Gohier, F.; Dabos-Seignon, S.; Breton, T.; Cougnon, C. A generic monolayer platform for the functionalization of surfaces through Sonogashira coupling. *Synthetic Metals* **2019**, *247*, 37-45. DOI: https://doi.org/10.1016/j.synthmet.2018.11.010.
(27) Gietter, A. A. S.; Pupillo, R. C.; Yap, G. P. A.; Beebe, T. P.; Rosenthal, J.; Watson, D. A. On-surface cross-coupling methods for the construction of modified electrode assemblies with tailored morphologies. *Chemical Science* **2013**, *4* (1), 437-443, 10.1039/C2SC21413J. DOI: 10.1039/C2SC21413J.
(28) Sheridan, M. V.; Lam, K.; Geiger, W. E. Spontaneous attachment of lithium-activated ferrocenylalkynes to carbon and gold. *Electrochemistry Communications* **2015**, *52*, 63-66. DOI: https://doi.org/10.1016/j.elecom.2015.01.024.
(29) Sheridan, M. V.; Lam, K.; Sharafi, M.; Schneebeli, S. T.; Geiger, W. E. Anodic Methods for Covalent Attachment of Ethynylferrocenes to Electrode Surfaces: Comparison of Ethynyl Activation Processes. *Langmuir* **2016**, *32* (6), 1645-1657. DOI: 10.1021/acs.langmuir.6b00012.
(30) Sheridan, M. V.; Lam, K.; Waterman, R.; Geiger, W. E. Anodic Oxidation of Ethynylferrocene Derivatives in Homogeneous Solution and Following Anodic Deposition onto Glassy Carbon Electrodes. *ChemElectroChem* **2019**, *6* (23), 5880-5887, https://doi.org/10.1002/celc.201901545. DOI: https://doi.org/10.1002/celc.201901545 (acccessed 2022/10/21).
(31) Gamm, P.; Sheridan, M. V.; Van Wyck, S. J.; Meindl, A.; Senge, M. O.; Geiger, W. E. Ethynylphenyl-Derivatized Free Base Porphyrins: Anodic Oxidation Processes and Covalent Grafting onto Glassy Carbon Electrodes. *Langmuir* **2020**, *36* (1), 96-108. DOI: 10.1021/acs.langmuir.9b03452.
(32) Zydziak, N.; Yameen, B.; Barner-Kowollik, C. Diels–Alder reactions for carbon material synthesis and surface functionalization. *Polymer Chemistry* **2013**, *4* (15), 4072-4086, 10.1039/C3PY00232B. DOI: 10.1039/C3PY00232B.
(33) Sarkar, S.; Bekyarova, E.; Haddon, R. C. Chemistry at the Dirac Point: Diels–Alder Reactivity of Graphene. *Accounts of Chemical Research* **2012**, *45* (4), 673-682. DOI: 10.1021/ar200302g.
(34) Kumar, I.; Rana, S.; Cho, J. W. Cycloaddition Reactions: A Controlled Approach for Carbon Nanotube Functionalization. *Chemistry – A European Journal* **2011**, *17* (40), 11092-11101, https://doi.org/10.1002/chem.201101260. DOI: https://doi.org/10.1002/chem.201101260 (acccessed 2022/10/21).
(35) Sarkar, S.; Bekyarova, E.; Niyogi, S.; Haddon, R. C. Diels−Alder Chemistry of Graphite and Graphene: Graphene as Diene and Dienophile. *Journal of the American Chemical Society* **2011**, *133* (10), 3324-3327. DOI: 10.1021/ja200118b.
(36) Munirasu, S.; Albuerne, J.; Boschetti-de-Fierro, A.; Abetz, V. Functionalization of Carbon Materials using the Diels-Alder Reaction. *Macromolecular Rapid Communications* **2010**, *31* (6),

574-579, https://doi.org/10.1002/marc.200900751. DOI: https://doi.org/10.1002/marc.200900751 (acccessed 2022/10/21).
(37) Zhang, W.; Sprafke, J. K.; Ma, M.; Tsui, E. Y.; Sydlik, S. A.; Rutledge, G. C.; Swager, T. M. Modular Functionalization of Carbon Nanotubes and Fullerenes. *Journal of the American Chemical Society* **2009**, *131* (24), 8446-8454. DOI: 10.1021/ja810049z.
(38) Bernal, M. M.; Liras, M.; Verdejo, R.; López-Manchado, M. A.; Quijada-Garrido, I.; París, R. Modification of carbon nanotubes with well-controlled fluorescent styrene-based polymers using the Diels–Alder reaction. *Polymer* **2011**, *52* (25), 5739-5745. DOI: https://doi.org/10.1016/j.polymer.2011.10.031.
(39) Al Dine, W. N.; Mehdi, A.; BouMalham, I.; Herro, Z.; Vioux, A.; Brun, N.; Fontaine, O. Self-Limited Grafting of Sub-Monolayers via Diels–Alder Reaction on Glassy Carbon Electrodes: An Electrochemical Insight. *ACS Omega* **2019**, *4* (24), 20540-20546. DOI: 10.1021/acsomega.9b02391.
(40) Kaper, H.; Grandjean, A.; Weidenthaler, C.; Schüth, F.; Goettmann, F. Surface Diels–Alder Reactions as an Effective Method to Synthesize Functional Carbon Materials. *Chemistry – A European Journal* **2012**, *18* (13), 4099-4106, https://doi.org/10.1002/chem.201102718. DOI: https://doi.org/10.1002/chem.201102718 (acccessed 2022/10/21).
(41) Fernandes, F. M.; Araújo, R.; Proença, M. F.; Silva, C. J. R.; Paiva, M. C. Functionalization of Carbon Nanofibers by a Diels-Alder Addition Reaction. *Journal of Nanoscience and Nanotechnology* **2007**, *7* (10), 3514-3518. DOI: 10.1166/jnn.2007.818.
(42) Farquhar, A. K.; Fitchett, C. M.; Dykstra, H. M.; Waterland, M. R.; Brooksby, P. A.; Downard, A. J. Diels–Alder Reaction of Anthranilic Acids: A Versatile Route to Dense Monolayers on Flat Edge and Basal Plane Graphitic Carbon Substrates. *ACS Applied Materials & Interfaces* **2016**, *8* (35), 23389-23395. DOI: 10.1021/acsami.6b07727.
(43) Le, C. M. Q.; Cao, X. T.; Tu, T. T. K.; Lee, W.-K.; Lim, K. T. Facile covalent functionalization of carbon nanotubes via Diels-Alder reaction in deep eutectic solvents. *Applied Surface Science* **2018**, *450*, 122-129. DOI: https://doi.org/10.1016/j.apsusc.2018.04.173.
(44) Delgado, J. L.; de la Cruz, P.; Langa, F.; Urbina, A.; Casado, J.; López Navarrete, J. T. Microwave-assisted sidewall functionalization of single-wall carbon nanotubes by Diels–Alder cycloaddition. *Chemical Communications* **2004**, (15), 1734-1735, 10.1039/B402375G. DOI: 10.1039/B402375G.
(45) Le, C. M. Q.; Cao, X. T.; Lim, K. T. Ultrasound-promoted direct functionalization of multi-walled carbon nanotubes in water via Diels-Alder "click chemistry". *Ultrasonics Sonochemistry* **2017**, *39*, 321-329. DOI: https://doi.org/10.1016/j.ultsonch.2017.04.042.
(46) Pobedinskas, P.; Degutis, G.; Dexters, W.; D'Haen, J.; Van Bael, M. K.; Haenen, K. Nanodiamond seeding on plasma-treated tantalum thin films and the role of surface contamination. *Applied Surface Science* **2021**, *538*, 148016. DOI: https://doi.org/10.1016/j.apsusc.2020.148016.
(47) Rodrigues, T.; Mishyn, V.; Leroux, Y. R.; Butruille, L.; Woitrain, E.; Barras, A.; Aspermair, P.; Happy, H.; Kleber, C.; Boukherroub, R.; et al. Highly performing graphene-based field effect transistor for the differentiation between mild-moderate-severe myocardial injury. *Nano Today* **2022**, *43*, 101391. DOI: https://doi.org/10.1016/j.nantod.2022.101391.
(48) Leroux, Y. R.; Hapiot, P. Nanostructured Monolayers on Carbon Substrates Prepared by Electrografting of Protected Aryldiazonium Salts. *Chemistry of Materials* **2013**, *25* (3), 489-495. DOI: 10.1021/cm303844v.

(49) Anariba, F.; DuVall, S. H.; McCreery, R. L. Mono- and Multilayer Formation by Diazonium Reduction on Carbon Surfaces Monitored with Atomic Force Microscopy "Scratching". *Analytical Chemistry* **2003**, *75* (15), 3837-3844. DOI: 10.1021/ac034026v.
(50) *Gwyddion Open Source Software*. http://gwyddion.net/ (accessed 11/03/2022).
(51) Reymond, S.; Cossy, J. Copper-Catalyzed Diels−Alder Reactions. *Chemical Reviews* **2008**, *108* (12), 5359-5406. DOI: 10.1021/cr078346g.
(52) Rowe, G. K.; Carter, M. T.; Richardson, J. N.; Murray, R. W. Consequences of Kinetic Dispersion on the Electrochemistry of an Adsorbed Redox-Active Monolayer. *Langmuir* **1995**, *11* (5), 1797-1806. DOI: 10.1021/la00005a059.
(53) Honeychurch, M. J. Effect of the Interfacial Potential Distribution on the Measurement of the Rate Constant for Electron Transfer between Electrodes and Redox Adsorbates. *Langmuir* **1998**, *14* (21), 6291-6296. DOI: 10.1021/la980150b.
(54) *ChemDraw Software*. https://perkinelmerinformatics.com/products/research/chemdraw (accessed 2021).
(55) Belu, A. M.; Graham, D. J.; Castner, D. G. Time-of-flight secondary ion mass spectrometry: techniques and applications for the characterization of biomaterial surfaces. *Biomaterials* **2003**, *24* (21), 3635-3653. DOI: https://doi.org/10.1016/S0142-9612(03)00159-5.
(56) Leroux, Y. R.; Bergamini, J.-F.; Ababou, S.; Le Breton, J.-C.; Hapiot, P. Synthesis of functionalized few-layer graphene through fast electrochemical expansion of graphite. *Journal of Electroanalytical Chemistry* **2015**, *753*, 42-46. DOI: https://doi.org/10.1016/j.jelechem.2015.06.013.
(57) Cançado, L. G.; Jorio, A.; Ferreira, E. H. M.; Stavale, F.; Achete, C. A.; Capaz, R. B.; Moutinho, M. V. O.; Lombardo, A.; Kulmala, T. S.; Ferrari, A. C. Quantifying Defects in Graphene via Raman Spectroscopy at Different Excitation Energies. *Nano Letters* **2011**, *11* (8), 3190-3196. DOI: 10.1021/nl201432g.

TOC graphic